Title

Existence of Pythagorean-hodograph quintic interpolants to spatial G 1 Hermite data with prescribed arc lengths

Author

Farouki, Rida T

Publication Date

2019-11-01

DOI

10.1016/j.jsc.2019.02.008

Peer reviewed

Existence of Pythagorean-hodograph quintic interpolants to spatial G^1 Hermite data with prescribed arc lengths

Rida T. Farouki
Department of Mechanical and Aerospace Engineering,
University of California, Davis, CA 95616, USA

Abstract

A unique feature of polynomial Pythagorean–hodograph (PH) curves is the ability to interpolate G^1 Hermite data (end points and tangents) with a specified total arc length. Since their construction involves the solution of a set of non–linear equations with coefficients dependent on the specified data, the existence of such interpolants in all instances is non–obvious. A comprehensive analysis of the existence of solutions in the case of spatial PH quintics with end derivatives of equal magnitude is presented, establishing that a two–parameter family of interpolants exists for any prescribed end points, end tangents, and total arc length. The two free parameters may be exploited to optimize a suitable shape measure of the interpolants, such as the elastic bending energy.

Keywords: geometric Hermite interpolation; Pythagorean–hodograph curves; arc length constraints; existence conditions; shape optimization; polynomial roots.

e–mail: farouki@ucdavis.edu

1 Introduction

The construction of spatial paths that satisfy specified boundary conditions (end points and tangents) and precisely achieve a desired total arc length is a fundamental problem in geometric design. Such problems may arise in robot path planning, carbon fiber layout in composites manufacturing, computer animation, path planning for unmanned or autonomous vehicles, and related applications. Polynomial Pythagorean–hodograph (PH) curves are uniquely suited to the construction of exact solutions to such problems, on account of the polynomial dependence of arc length on the curve parameter [5].

The construction of curved paths with prescribed arc lengths satisfying given boundary conditions has thus far received relatively little attention. A closed–form solution to the problem of interpolating planar G^1 Hermite data under arc length constraints was developed in [6], using planar PH quintics, and in [11] a numerical scheme was employed to solve the system of non–linear equations that define a spatial C^2 PH quintic spline interpolating a sequence of nodal points with specified internodal arc lengths. The paper [12] provides a closed–form solution to the problem of interpolating spatial G^1 data using rational PH curves of class 4 (degree ≤ 6) with prescribed arc lengths. This result, however, is not representative of all rational PH space curves — which do not, in general, admit rational arc length functions.

The focus of the present study[1] is on generalizing the results of [6] from planar to spatial PH quintics. This is a non–trivial problem, since spatial PH curves require more sophisticated algebraic models — namely, the quaternion or Hopf map formulations [4] — to ensure invariance under spatial rotations [7]. A detailed analysis of the system of non–linear equations that express the interpolation of initial/final points $\mathbf{p}_i, \mathbf{p}_f$ and tangents $\mathbf{t}_i, \mathbf{t}_f$ and a total arc length S is required, to establish the existence of interpolants for all instances of these data. Moreover, an infinitude of solutions is obtained, rather than a finite number of distinct interpolants as in the planar case.

The problem of interpolating spatial G^1 Hermite data by quintic PH space curves of prescribed arc length can be reduced to finding the real solutions of a system of non–linear equations, whose coefficients depend on the specified data (end points/tangents, and total arc length), and it is not obvious *a priori* that real solutions exist for all possible data sets. The analysis developed here verifies the existence of interpolants in all instances, and also shows that they

[1] We focus here on solutions to the interpolation problem using single PH quintic curve segments. However, the methods should be adaptable to 'biarcs" (i.e., interpolants defined by two PH curve segments that meet with a prescribed order of geometric continuity).

comprise a two–parameter family, incorporating two free variables that may be exploited to optimize the shape of the interpolant. In the present context, the Hopf map representation is found to be most convenient for the existence proof, and a key element in rendering the analysis tractable is the adoption of a *canonical form*, corresponding to a particular choice of coordinate system. For the actual construction of interpolants, the quaternion form is preferable.

The remainder of this paper is organized as follows. A brief review of the quaternion and Hopf map representations of spatial PH curves is presented in Section 2, and the latter is used to formulate the basic problem of achieving a given end–point displacement subject to a prescribed total arc length. For the case of spatial PH quintics, Section 3 develops a comprehensive analysis of the existence of solutions to the interpolation of spatial G^1 Hermite under an arc length constraint, which is reduced to showing that one of the roots of a biquadratic equation with data–dependent coefficients always satisfies two data–dependent upper bounds. Section 4 exploits the results of this analysis to formulate an algorithm to construct the interpolants, and briefly discusses use of the free parameters they incorporate to optimize appropriate shape measures. Finally, Section 5 summarizes the main results of this study, and suggests avenues for further possible investigation.

It should be noted that a number of the results presented herein may prove rather challenging as "pencil–and–paper" derivations — the `Maple` computer algebra has been used in several instances to derive or verify them.

2 Spatial Pythagorean-hodograph curves

The *quaternion* and *Hopf map* forms [4, 7] are alternative (equivalent) models for the construction of spatial PH curves. The former generates a Pythagorean hodograph $\mathbf{r}'(\xi)$ from a quaternion[2] polynomial

$$\mathcal{A}(\xi) \;=\; u(\xi) + v(\xi)\,\mathbf{i} + p(\xi)\,\mathbf{j} + q(\xi)\,\mathbf{k} \tag{1}$$

and its conjugate $\mathcal{A}^*(\xi) = u(\xi) - v(\xi)\,\mathbf{i} - p(\xi)\,\mathbf{j} - q(\xi)\,\mathbf{k}$ through the product[3]

$$\begin{aligned}\mathbf{r}'(\xi) \;=\; \mathcal{A}(\xi)\,\mathbf{i}\,\mathcal{A}^*(\xi) \;=\; & [\,u^2(\xi) + v^2(\xi) - p^2(\xi) - q^2(\xi)\,]\,\mathbf{i} \\ & + 2\,[\,u(\xi)q(\xi) + v(\xi)p(\xi)\,]\,\mathbf{j} \;+\; 2\,[\,v(\xi)q(\xi) - u(\xi)p(\xi)\,]\,\mathbf{k}\,, \end{aligned} \tag{2}$$

[2]Calligraphic characters such as $\mathcal{A}$ are used to denote quaternions, their scalar (real) and vector (imaginary) parts being denoted by $\mathrm{scal}(\mathcal{A})$ and $\mathrm{vect}(\mathcal{A})$. Bold symbols denote either complex numbers or vectors in $\mathbb{R}^3$ — the meaning should be clear from the context.

[3]Note that products of the form $\mathcal{A}\,\mathbf{i}\,\mathcal{A}^*$ always generate pure vector quaternions.

and the latter generates a Pythagorean hodograph from complex polynomials

$$\boldsymbol{\alpha}(\xi) \;=\; u(\xi) + \mathrm{i}\, v(\xi)\,, \quad \boldsymbol{\beta}(\xi) \;=\; q(\xi) + \mathrm{i}\, p(\xi) \tag{3}$$

through the expression

$$\mathbf{r}'(\xi) \;=\; (|\boldsymbol{\alpha}(\xi)|^2 - |\boldsymbol{\beta}(\xi)|^2, 2\,\mathrm{Re}(\boldsymbol{\alpha}(\xi)\overline{\boldsymbol{\beta}}(\xi)), 2\,\mathrm{Im}(\boldsymbol{\alpha}(\xi)\overline{\boldsymbol{\beta}}(\xi)))\,. \tag{4}$$

The parametric speed (i.e., the derivative $\mathrm{d}s/\mathrm{d}\xi$ of arc length s with respect to the curve parameter ξ) is defined in these two representations by

$$\sigma(\xi) \;=\; |\mathbf{r}'(\xi)| \;=\; |\mathcal{A}(\xi)|^2 \;=\; |\boldsymbol{\alpha}(\xi)|^2 + |\boldsymbol{\beta}(\xi)|^2\,.$$

The equivalence of (2) and (4) is seen by taking $\mathcal{A}(\xi) = \boldsymbol{\alpha}(\xi) + \mathbf{k}\,\boldsymbol{\beta}(\xi)$, where the imaginary unit i is identified with the quaternion basis element $\mathbf{i}$.

Since the PH curve $\mathbf{r}(\xi)$ is obtained by integration of (2) or (4), the initial point $\mathbf{r}(0) = \mathbf{p}_i$ may always be freely specified as the integration constant. It is advantageous to simultaneously use both of the representations (2) and (4) — the Hopf map form yields a simpler expression of the arc length constraint in the existence proof, but the quaternion form is somewhat more convenient in formulating an algorithm to construct the interpolants.

We wish to study the existence of spatial PH curves $\mathbf{r}(\xi)$, $\xi \in [\,0, 1\,]$ with given initial and final points $\mathbf{p}_i, \mathbf{p}_f$ and unit tangents $\mathbf{t}_i, \mathbf{t}_f$ and specified total arc length $S > |\,\Delta\mathbf{p}\,|$, where $\Delta\mathbf{p} = \mathbf{p}_f - \mathbf{p}_i$. To define a true space curve, the given data must not be coplanar, i.e., it must satisfy the condition

$$(\mathbf{t}_i \times \mathbf{t}_f) \cdot \Delta\mathbf{p} \;\neq\; 0\,. \tag{5}$$

The planar case of this problem has been previously addressed in [6].

Setting $\Delta\mathbf{p} = (\Delta x, \Delta y, \Delta z)$ and invoking the Hopf map form defined by (3)–(4), satisfaction of the end–point displacement yields the real equation

$$\int_0^1 |\boldsymbol{\alpha}(\xi)|^2 - |\boldsymbol{\beta}(\xi)|^2\,\mathrm{d}\xi \;=\; \Delta x\,, \tag{6}$$

together with the complex equation

$$\int_0^1 2\,\boldsymbol{\alpha}(\xi)\overline{\boldsymbol{\beta}}(\xi)\,\mathrm{d}\xi \;=\; \Delta y + \mathrm{i}\,\Delta z\,, \tag{7}$$

while satisfaction of the specified arc length yields the real equation

$$\int_0^1 |\boldsymbol{\alpha}(\xi)|^2 + |\boldsymbol{\beta}(\xi)|^2\,\mathrm{d}\xi \;=\; S\,. \tag{8}$$

Equations (6) and (8) may be combined to obtain the simpler conditions

$$\int_0^1 |\boldsymbol{\alpha}(\xi)|^2\,\mathrm{d}\xi \;=\; \tfrac{1}{2}(S + \Delta x) \quad \text{and} \quad \int_0^1 |\boldsymbol{\beta}(\xi)|^2\,\mathrm{d}\xi \;=\; \tfrac{1}{2}(S - \Delta x)\,. \tag{9}$$

3 Existence of PH quintic interpolants

We focus henceforth on the case of spatial PH quintics, generated by complex quadratic polynomials specified in Bernstein form as

$$\begin{aligned} \boldsymbol{\alpha}(\xi) &= \boldsymbol{\alpha}_0(1-\xi)^2 + \boldsymbol{\alpha}_1 2(1-\xi)\xi + \boldsymbol{\alpha}_2\xi^2\,, \\ \boldsymbol{\beta}(\xi) &= \boldsymbol{\beta}_0(1-\xi)^2 + \boldsymbol{\beta}_1 2(1-\xi)\xi + \boldsymbol{\beta}_2\xi^2\,. \end{aligned} \tag{10}$$

Equation (7) then reduces to

$$\begin{aligned} &6\,\boldsymbol{\alpha}_0\overline{\boldsymbol{\beta}}_0 + 3\,\boldsymbol{\alpha}_0\overline{\boldsymbol{\beta}}_1 + 3\,\boldsymbol{\alpha}_1\overline{\boldsymbol{\beta}}_0 + \boldsymbol{\alpha}_0\overline{\boldsymbol{\beta}}_2 + \boldsymbol{\alpha}_2\overline{\boldsymbol{\beta}}_0 \\ &\quad + 4\,\boldsymbol{\alpha}_1\overline{\boldsymbol{\beta}}_1 + 3\,\boldsymbol{\alpha}_1\overline{\boldsymbol{\beta}}_2 + 3\,\boldsymbol{\alpha}_2\overline{\boldsymbol{\beta}}_1 + 6\,\boldsymbol{\alpha}_2\overline{\boldsymbol{\beta}}_2 \;=\; 30\,(\Delta y + \mathrm{i}\,\Delta z)\,, \end{aligned}$$

while equations (9) become

$$\begin{aligned} &6\,|\boldsymbol{\alpha}_0|^2 + 6\,\mathrm{Re}(\boldsymbol{\alpha}_0\overline{\boldsymbol{\alpha}}_1) + 2\,\mathrm{Re}(\boldsymbol{\alpha}_0\overline{\boldsymbol{\alpha}}_2) \\ &\qquad + 4\,|\boldsymbol{\alpha}_1|^2 + 6\,\mathrm{Re}(\boldsymbol{\alpha}_1\overline{\boldsymbol{\alpha}}_2) + 6\,|\boldsymbol{\alpha}_2|^2 \;=\; 15\,(S + \Delta x)\,, \\ &6\,|\boldsymbol{\beta}_0|^2 + 6\,\mathrm{Re}(\boldsymbol{\beta}_0\overline{\boldsymbol{\beta}}_1) + 2\,\mathrm{Re}(\boldsymbol{\beta}_0\overline{\boldsymbol{\beta}}_2) \\ &\qquad + 4\,|\boldsymbol{\beta}_1|^2 + 6\,\mathrm{Re}(\boldsymbol{\beta}_1\overline{\boldsymbol{\beta}}_2) + 6\,|\boldsymbol{\beta}_2|^2 \;=\; 15\,(S - \Delta x)\,. \end{aligned}$$

To facilitate the analysis, we adopt a *canonical form* coordinate system[4] in which $(\Delta x, \Delta y, \Delta z) = (1, 0, 0)$. Then by straightforward but rather laborious calculations, the preceding equations can be re–formulated as

$$\begin{aligned} &[\,4\,\boldsymbol{\alpha}_1 + 3\,(\boldsymbol{\alpha}_0 + \boldsymbol{\alpha}_2)\,]\,[\,4\,\overline{\boldsymbol{\beta}}_1 + 3\,(\overline{\boldsymbol{\beta}}_0 + \overline{\boldsymbol{\beta}}_2)\,] \\ &\qquad = 5\,[\,\boldsymbol{\alpha}_0\overline{\boldsymbol{\beta}}_2 + \boldsymbol{\alpha}_2\overline{\boldsymbol{\beta}}_0 - 3\,(\boldsymbol{\alpha}_0\overline{\boldsymbol{\beta}}_0 + \boldsymbol{\alpha}_2\overline{\boldsymbol{\beta}}_2)\,]\,, \end{aligned} \tag{11}$$

$$\begin{aligned} &|\,4\,\boldsymbol{\alpha}_1 + 3\,(\boldsymbol{\alpha}_0 + \boldsymbol{\alpha}_2)\,|^2 \\ &\qquad = 5\,[\,12\,(S+1) - 2\,(|\boldsymbol{\alpha}_0|^2 + |\boldsymbol{\alpha}_2|^2) - |\boldsymbol{\alpha}_0 - \boldsymbol{\alpha}_2|^2\,]\,, \end{aligned} \tag{12}$$

$$\begin{aligned} &|\,4\,\boldsymbol{\beta}_1 + 3\,(\boldsymbol{\beta}_0 + \boldsymbol{\beta}_2)\,|^2 \\ &\qquad = 5\,[\,12\,(S-1) - 2\,(|\boldsymbol{\beta}_0|^2 + |\boldsymbol{\beta}_2|^2) - |\boldsymbol{\beta}_0 - \boldsymbol{\beta}_2|^2\,]\,. \end{aligned} \tag{13}$$

Note that these equations depend on the specified arc length S, and they are also inter–dependent. In order for equations (12) and (13) to admit solutions, we must have

$$2\,(|\boldsymbol{\alpha}_0|^2 + |\boldsymbol{\alpha}_2|^2) \;+\; |\boldsymbol{\alpha}_0 - \boldsymbol{\alpha}_2|^2 \;\le\; 12\,(S+1)\,, \tag{14}$$

$$2\,(|\boldsymbol{\beta}_0|^2 + |\boldsymbol{\beta}_2|^2) \;+\; |\boldsymbol{\beta}_0 - \boldsymbol{\beta}_2|^2 \;\le\; 12\,(S-1)\,. \tag{15}$$

[4] Arbitrary given curve data $\mathbf{p}_i, \mathbf{p}_f, \mathbf{t}_i, \mathbf{t}_f, S$ can be mapped to canonical form through a scaling/rotation transformation.

Moreover, for equations (12) and (13) to be consistent with equation (11), we must also have

$$\begin{aligned} &| \boldsymbol{\alpha}_0\overline{\boldsymbol{\beta}}_2 + \boldsymbol{\alpha}_2\overline{\boldsymbol{\beta}}_0 - 3\,(\boldsymbol{\alpha}_0\overline{\boldsymbol{\beta}}_0 + \boldsymbol{\alpha}_2\overline{\boldsymbol{\beta}}_2)\,|^2 \\ &\qquad = [\,12\,(S+1) - 2\,(|\boldsymbol{\alpha}_0|^2 + |\boldsymbol{\alpha}_2|^2) - |\boldsymbol{\alpha}_0 - \boldsymbol{\alpha}_2|^2\,] \\ &\qquad\quad \cdot\ [\,12\,(S-1) - 2\,(|\boldsymbol{\beta}_0|^2 + |\boldsymbol{\beta}_2|^2) - |\boldsymbol{\beta}_0 - \boldsymbol{\beta}_2|^2\,]\,. \end{aligned} \tag{16}$$

Equations (11)–(13) may be interpreted as determining $\boldsymbol{\alpha}_1, \boldsymbol{\beta}_1$ in terms of $\boldsymbol{\alpha}_0, \boldsymbol{\beta}_0$ and $\boldsymbol{\alpha}_2, \boldsymbol{\beta}_2$ when the latter are specified in terms of certain free (real) parameters, as elaborated below. Equations (12) and (13) identify $\boldsymbol{\alpha}_1, \boldsymbol{\beta}_1$ as lying on circles in the complex plane, when conditions (14)–(15) are satisfied. If either $\boldsymbol{\alpha}_1$ or $\boldsymbol{\beta}_1$ is chosen as a point on the appropriate circle, and condition (16) is satisfied, the other may be uniquely determined from (11).

The end tangents $\mathbf{t}_i$ and $\mathbf{t}_f$ are specified in terms of polar and azimuthal angles (θ_i, ϕ_i) and (θ_f, ϕ_f) relative to the x–axis as

$$\begin{aligned} \mathbf{t}_i &= (\cos\theta_i, \sin\theta_i\cos\phi_i, \sin\theta_i\sin\phi_i)\,, \\ \mathbf{t}_f &= (\cos\theta_f, \sin\theta_f\cos\phi_f, \sin\theta_f\sin\phi_f)\,, \end{aligned} \tag{17}$$

where $\theta_i, \theta_f \in [\,0, \pi\,]$ and $\phi_i, \phi_f \in [\,0, 2\pi)$. With $\Delta\mathbf{p} = (1, 0, 0)$ the condition (5) for the given data to be non–planar then becomes

$$\sin\theta_i\,\sin\theta_f\,\sin\Delta\phi \;\neq\; 0\,, \tag{18}$$

with $\Delta\phi = \phi_f - \phi_i$, i.e., θ_i and θ_f must not be equal to 0 or π, and ϕ_i and ϕ_f must not differ by an integer multiple of π.

To ensure that symmetric data yields symmetric interpolants, we assume end derivatives of equal magnitude, i.e., $|\mathbf{r}'(0)| = |\mathbf{r}'(1)| = w^2$ with $w \neq 0$. In order to match the end tangents $(\boldsymbol{\alpha}_0, \boldsymbol{\beta}_0)$ and $(\boldsymbol{\alpha}_2, \boldsymbol{\beta}_2)$ must satisfy

$$\frac{|\boldsymbol{\alpha}_0|^2 - |\boldsymbol{\beta}_0|^2}{|\boldsymbol{\alpha}_0|^2 + |\boldsymbol{\beta}_0|^2} = \cos\theta_i\,, \quad \frac{2\,\boldsymbol{\alpha}_0\overline{\boldsymbol{\beta}}_0}{|\boldsymbol{\alpha}_0|^2 + |\boldsymbol{\beta}_0|^2} = \sin\theta_i\exp(\mathrm{i}\,\phi_i)\,,$$

$$\frac{|\boldsymbol{\alpha}_2|^2 - |\boldsymbol{\beta}_2|^2}{|\boldsymbol{\alpha}_2|^2 + |\boldsymbol{\beta}_2|^2} = \cos\theta_f\,, \quad \frac{2\,\boldsymbol{\alpha}_2\overline{\boldsymbol{\beta}}_2}{|\boldsymbol{\alpha}_2|^2 + |\boldsymbol{\beta}_2|^2} = \sin\theta_f\exp(\mathrm{i}\,\phi_f)\,,$$

and consequently one can verify that they must be of the form

$$\boldsymbol{\alpha}_0 = w\,c_i\exp(\mathrm{i}\,\phi_i)\exp(\mathrm{i}\,\psi_0)\,, \quad \boldsymbol{\beta}_0 = w\,s_i\exp(\mathrm{i}\,\psi_0)\,, \tag{19}$$

$$\boldsymbol{\alpha}_2 = w\,c_f\exp(\mathrm{i}\,\phi_f)\exp(\mathrm{i}\,\psi_2)\,, \quad \boldsymbol{\beta}_2 = w\,s_f\exp(\mathrm{i}\,\psi_2)\,, \tag{20}$$

where ψ_0, ψ_2 are free parameters,[5] and for brevity we write

$$(c_i, s_i) \;=\; (\cos\tfrac{1}{2}\theta_i, \sin\tfrac{1}{2}\theta_i) \quad \text{and} \quad (c_f, s_f) \;=\; (\cos\tfrac{1}{2}\theta_f, \sin\tfrac{1}{2}\theta_f)\,. \tag{21}$$

Note that $0 < c_i, s_i, c_f, s_f < 1$ to satisfy the non–planar data condition (18).

Setting $\Delta\psi = \psi_2 - \psi_0$, the inequalities (14)–(15) yield

$$w^2 \;\le\; k_1 \;:=\; \frac{12(S+1)}{f}\,, \quad w^2 \;\le\; k_2 \;:=\; \frac{12(S-1)}{g}\,, \tag{22}$$

where we define

$$f \;:=\; 3(c_i^2 + c_f^2) - 2\,c_i c_f \cos(\Delta\phi + \Delta\psi)\,, \tag{23}$$

$$g \;:=\; 3(s_i^2 + s_f^2) - 2\,s_i s_f \cos\Delta\psi\,. \tag{24}$$

Note that k_1 may be smaller than or larger than k_2, depending on the values of $S, \theta_i, \theta_f, \Delta\phi, \Delta\psi$.

Lemma 1. *For $1 < S < \infty$ and non–planar data satisfying* (18)*, the bounds* (22) *on w^2 are both positive and finite.*

Proof : For $1 < S < \infty$, the numerators in the expressions (22) for k_1, k_2 are positive and finite. Recalling that $0 < c_i, s_i, c_f, s_f < 1$ for non–planar data, the denominators are also seen to be positive and finite by re–writing them:

$$f \;=\; 2\,(c_i^2 + c_f^2) + (c_i - c_f)^2 + 2\,c_i c_f\,[\,1 - \cos(\Delta\phi + \Delta\psi)\,] \;>\; 0\,, \tag{25}$$

$$g \;=\; 2\,(s_i^2 + s_f^2) + (s_i - s_f)^2 + 2\,s_i s_f\,[\,1 - \cos\Delta\psi\,] \;>\; 0\,. \tag{26}$$

Hence the bounds k_1, k_2 on w^2 are positive and finite. ∎

Now substituting from (19) and (20), the condition (16) may be reduced to the biquadratic equation

$$p(w^2) \;:=\; c_2 w^4 + c_1 w^2 + c_0 \;=\; 0 \tag{27}$$

in w, with coefficients expressed (after considerable simplification) as

$$c_2 \;:=\; 2\,(c_i^2 s_f^2 + s_i^2 c_f^2) - 4\,c_i s_i c_f s_f \cos\Delta\phi\,, \tag{28}$$

$$\begin{aligned} c_1 \;:=\; & 6\,[\,(S-1)c_i c_f \cos(\Delta\phi + \Delta\psi) + (S+1)s_i s_f \cos\Delta\psi - 3\,S\,] \\ & + 9\,(c_i^2 - s_i^2 + c_f^2 - s_f^2)\,, \end{aligned} \tag{29}$$

$$c_0 \;:=\; 36\,(S^2 - 1)\,. \tag{30}$$

[5]The parameters ψ_0 and ψ_2 determine the orientation of normal–plane vectors of the *Euler–Rodrigues frame* [3] at the curve end points, and they also influence the curve shape.

Remark 1. The above analysis may be seen to generalize the planar problem treated in [6] as follows. For planar data, using a coordinate system in which the curve lies within the (x, y) plane corresponds to azimuthal tangent angles $\phi_i = \phi_f = 0$ in (17), so $\Delta\phi = 0$. Furthermore, we set $\psi_0 = \psi_2 = 0$ and thus $\Delta\psi = 0$, since the complex representation of planar PH curves does not incur the free angular parameters ψ_0, ψ_2. One can then verify that the coefficients (28)–(30) of equation (27) are identical to the coefficients of the analogous biquadratic equation in Proposition 2 of [6].

Clearly, c_0 is positive when $S > 1$. Moreover, using equations (22)–(24), the coefficient c_1 can be re–formulated as

$$c_1 \;=\; -\,36\,(S^2-1)\left[\,\frac{1}{k_1}+\frac{1}{k_2}\,\right]. \tag{31}$$

Hence, by Lemma 1, c_1 is always negative for non–planar data. Finally, we can also ascertain the sign of the coefficient c_2 as follows.

Lemma 2. *For non–planar data satisfying* (18)*, c_2 is always positive.*

Proof : To verify that c_2 is always positive when condition (18) holds, we re–write it as

$$c_2 \;=\; 2\,(c_i s_f - c_f s_i)^2 + 4\,c_i s_i c_f s_f (1-\cos\Delta\phi)\,. \tag{32}$$

Since $0 \le c_i, s_i, c_f, s_f \le 1$ for $\theta_i, \theta_f \in [\,0, \pi\,]$, this expression is evidently non–negative, and $c_2 = 0$ if and only if $c_i s_f - c_f s_i = 0$ and $4\,c_i s_i c_f s_f (1-\cos\Delta\phi) = 0$. Now from (21) we have $c_i s_f - c_f s_i = \sin\frac{1}{2}(\theta_f - \theta_i)$ and $4\,c_i s_i c_f s_f = \sin\theta_i \sin\theta_f$. Therefore, the first condition implies that $\theta_f = \theta_i$, and the second then implies that either $\sin\theta_i = \sin\theta_f = 0$ or $\cos\Delta\phi = 1$ (i.e., $\sin\Delta\phi = 0$), which violate the non–planar condition (18). Thus, the expression (32) vanishes only when $\theta_i, \theta_f, \Delta\phi$ define planar data, and is otherwise always positive. ∎

Hence, when condition (18) is satisfied, the coefficients c_2, c_1, c_0 exhibit two sign changes, and by Descartes' Law of Signs [15] the number of positive real roots w^2 of (27) is zero or two. To guarantee that an interpolant exists,[6] this equation must have a positive root w^2 that satisfies the inequalities (22). Note that if w_1^2 and w_2^2 are the roots of (27), they must satisfy

$$w_1^2 + w_2^2 \;=\; \frac{36(S^2-1)}{c_2}\left[\,\frac{1}{k_1}+\frac{1}{k_2}\,\right] \quad \text{and} \quad w_1^2 w_2^2 \;=\; \frac{36(S^2-1)}{c_2}\,, \tag{33}$$

[6]Note that the inequalities (22) and equation (27) depend only on the differences $\Delta\phi$ and $\Delta\psi$, and not individually on ϕ_i, ϕ_f and ψ_0, ψ_2.

and hence the harmonic mean of w_1^2 and w_2^2 is equal to that of k_1 and k_2, i.e.,

$$\frac{1}{w_1^2} + \frac{1}{w_2^2} \;=\; \frac{1}{k_1} + \frac{1}{k_2}\,. \tag{34}$$

To determine the nature of the roots w_1^2 and w_2^2, and their locations relative to k_1 and k_2, we need the following result.

Lemma 3. *For non–planar data satisfying* (18)*, $4\,c_2 - fg$ is non–positive.*

Proof : Using the `Maple` function `extrema` and considering c_i, s_i, c_f, s_f as fixed symbols, the maximum values of $4\,c_2 - fg$ with respect to $\Delta\phi$ and $\Delta\psi$ were determined. Since `extrema` can only work on algebraic expressions, this was accomplished by treating $\cos\Delta\phi, \sin\Delta\phi, \cos\Delta\psi, \sin\Delta\psi$ as four variables subject to the constraints $\cos^2\Delta\phi + \sin^2\Delta\phi = 1$ and $\cos^2\Delta\psi + \sin^2\Delta\psi = 1$. The `extrema` function returns $\max(e_1, e_2, e_3, e_4, e_5, e_6)$ where $e_1, \ldots, e_4$ can be expressed, with corresponding $\Delta\phi, \Delta\psi$ values, as the factored forms

$$\begin{aligned}
e_1 \;&=\; -\left(c_i s_f + s_i c_f - 3\,c_i s_i - 3\,c_f s_f\right)^2, \quad (\Delta\phi, \Delta\psi) = (0, 0)\,,\\
e_2 \;&=\; -\left(c_i s_f - s_i c_f - 3\,c_i s_i + 3\,c_f s_f\right)^2, \quad (\Delta\phi, \Delta\psi) = (\pi, 0)\,,\\
e_3 \;&=\; -\left(c_i s_f + s_i c_f + 3\,c_i s_i + 3\,c_f s_f\right)^2, \quad (\Delta\phi, \Delta\psi) = (0, \pi)\,,\\
e_4 \;&=\; -\left(c_i s_f - s_i c_f + 3\,c_i s_i - 3\,c_f s_f\right)^2, \quad (\Delta\phi, \Delta\psi) = (\pi, \pi)\,.
\end{aligned}$$

The remaining two cases are specified by $e_5 = 0$ together with

$$\cos\Delta\phi \;=\; \frac{9\,(c_i^2 s_f^2 + s_i^2 c_f^2) - 8}{18\,c_i s_i c_f s_f}\,, \quad \cos\Delta\psi \;=\; \frac{9\,(s_i^2 + s_f^2) - 8}{6\,s_i s_f}\,, \tag{35}$$

and $e_6 = 8\,(c_f^2 - c_i^2)^2$ together with

$$\cos\Delta\phi \;=\; \frac{(c_f^2 - c_i^2)^2 + 7\,(c_i^2 s_f^2 + s_i^2 c_f^2) - 8}{18\,c_i s_i c_f s_f}\,, \quad \cos\Delta\psi \;=\; \frac{8 + s_i^2 + s_f^2}{6\,s_i s_f}\,. \tag{36}$$

The corresponding values for $\sin\Delta\phi$ and $\sin\Delta\psi$ are indeterminate in sign.

Note that e_1, e_3 vanish when

$$\sin\tfrac{1}{2}(\theta_i + \theta_f) \;=\; \pm\,\frac{3}{2}\,(\sin\theta_i + \sin\theta_f)\,. \tag{37}$$

On the other hand e_2, e_4 vanish when

$$\sin\tfrac{1}{2}(\theta_f - \theta_i) \;=\; \pm\,\frac{3}{2}\,(\sin\theta_i - \sin\theta_f)\,, \tag{38}$$

and in particular when $\theta_i = \theta_f$, but these instances with $\Delta\phi = \pi$ correspond to degenerate cases, violating the non–planarity condition (18).

The case e_5 is singular, corresponding to a double root for equation (27), and the expressions for $\cos\Delta\phi$ and $\cos\Delta\psi$ are only valid over restricted ranges of θ_i and θ_f. In this case, we have $c_2 = 16/9$ and $g = 8/3$, but the expression for f contains irreducible radical terms in c_i, s_i, c_f, s_f. It can be verified that $4\,c_2 - fg$ vanishes only for the values

$$(c_i, s_i) \;=\; (c_f, s_f) \;=\; (3/5, 4/5)\,, \tag{39}$$

$$(c_i, s_i) \;=\; (c_f, s_f) \;=\; (4/5, 3/5)\,, \tag{40}$$

$$(c_i, s_i) \;=\; (3/5, 4/5)\,, \quad (c_f, s_f) \;=\; (4/5, 3/5)\,, \tag{41}$$

$$(c_i, s_i) \;=\; (4/5, 3/5)\,, \quad (c_f, s_f) \;=\; (3/5, 4/5)\,, \tag{42}$$

provided that $\sin\Delta\phi$ and $\sin\Delta\psi$ are of the same sign. Finally, e_6 identifies an invalid extremum arising from the fact that, although c_i, s_i, c_f, s_f must be greater than 0 and less than 1 for satisfaction of the non–planarity condition (18), they are treated as unconstrained quantities in the computation. Since, in this case, the expression for $\cos\Delta\psi$ in (36) yields

$$\cos\Delta\psi \;=\; \frac{8 + s_i^2 + s_f^2}{6\,s_i s_f} \;>\; \frac{4}{3}\,,$$

which is impossible, the case e_6 is discarded. In summary, since e_1, e_2, e_3, e_4, e_5 are always non–positive for non–planar data, and e_6 is invalid, the quantity $4\,c_2 - fg$ is always non–positive. ■

The preceding Lemma will now be used to analyze the roots of equation (27), and their relationship with the bounds k_1 and k_2 defined in (22).

Proposition 1. *For non–planar data $\theta_i, \theta_f, \phi_i, \phi_f, S$ satisfying* (18) *and each value of the parameter $\Delta\psi$, the equation* (27) *has in general two positive real roots w^2 of which only the smaller root satisfies the inequalities* (22).

Proof : By "in general" we mean that none of the singular conditions causing the quantities e_1, e_2, e_3, e_4, e_5 in Lemma 3 to vanish are satisfied. Specifically,

- e_1, e_3: when $(\Delta\phi, \Delta\psi) = (0, 0)$ or $(0, \pi)$ condition (37) does not hold;
- e_2, e_4: when $(\Delta\phi, \Delta\psi) = (\pi, 0)$ or (π, π) condition (38) does not hold;
- e_5: $\Delta\phi$ and $\Delta\psi$ do not satisfy (35) together with the values (39)–(42).

Under these restrictions, the quantity $4\,c_2 - f\,g$ is always negative.

As noted above, the signs of the coefficients (28)–(30) indicate that the biquadratic equation (27) has either zero or two positive real roots. Since a direct evaluation of the discriminant proves rather cumbersome, we invoke an indirect argument to verify that the latter case always holds.

Noting from (25) and (26) that $f \neq 0$ and $g \neq 0$ for non–planar data, and using (22), (23)–(24), and (31), we obtain the expressions

$$p(k_1) \;=\; \frac{36(S+1)^2}{f^2}\,(4\,c_2 - f\,g)\,, \quad p(k_2) \;=\; \frac{36(S-1)^2}{g^2}\,(4\,c_2 - f\,g)\,,$$

for (27) evaluated at $w^2 = k_1$ and $w^2 = k_2$. Thus, $p(k_1)$ and $p(k_2)$ must both be negative, since $4\,c_2 - f\,g$ is negative. Since $p(0) = c_0 > 0$ and $p(w^2) > 0$ as $w^2 \to \infty$, and k_1 and k_2 are both positive, this implies that (27) must have two positive real roots, which satisfy the conditions (34).

Consider now how the roots w_1^2 and w_2^2 are situated relative to the bounds k_1, k_2 defined by (22). We assume, without loss of generality, that $w_1^2 < w_2^2$, so the graph of $p(w^2)$ is positive for $0 < w^2 < w_1^2$, negative for $w_1^2 < w^2 < w_2^2$, and positive for $w_2^2 < w^2 < \infty$ (see Figure 1). Then, since $p(k_1)$ and $p(k_2)$ are negative, k_1 and k_2 must lie between w_1^2 and w_2^2, i.e., w_1^2 must be less than both k_1 and k_2, while w_2^2 must be greater than both k_1 and k_2, as indicated in Figure 1. Hence, w_1^2 satisfies the bounds (22) but w_2^2 does not. ∎

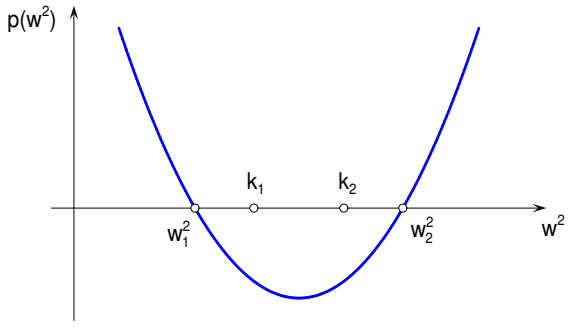

Figure 1: Schematic graph of the function (27), illustrating the location of its roots w_1^2 and w_2^2 in relation to the two points k_1 and k_2 defined by (22) — note that k_1 may be either less than or greater than k_2.

The upshot of the preceding analysis is that, to achieve a prescribed arc length S in the interpolation of G^1 Hermite data by spatial PH quintics, the

common end derivative magnitude $w^2 = |\mathbf{r}'(0)| = |\mathbf{r}'(1)|$ must be determined as the smaller root of the equation (27), with coefficients (28)–(30) dependent on S, the angular variables $\theta_i, \theta_f, \phi_i, \phi_f$ that specify end tangents consistent with the non–planarity condition (18), and the difference $\Delta\psi = \psi_2 - \psi_0$ of the free parameters ψ_0 and ψ_2 in expressions (19) and (20).

We summarize the outcome of all the preceding discussions as follows.

Theorem 1. *For any $S > 1$ and end tangent data $\theta_i, \theta_f, \phi_i, \phi_f$ satisfying the non–planar condition* (18)*, the canonical–form G^1 spatial PH quintic Hermite interpolation problem with end point displacement $\Delta\mathbf{p} = (1, 0, 0)$ admits a two–parameter family of solutions with precise arc lengths S, dependent on the angular variables ψ_0, ψ_2 introduced in* (19)–(20)*.*

Note that this result also encompasses, as a limiting case, the degenerate instances in which equation (27) possesses a double root, corresponding to the coincidences $4\,c_2 - f\,g = 0$ and $w_1^2 = w_2^2 = k_1 = k_2$.

4 Algorithm and computed examples

Having established the existence of solutions for arbitrary non–planar data, we now consider their construction. In this context, it is convenient to employ the quaternion form (2), since this allows us to exploit existing methodology [8, 9] for Hermite interpolation by spatial PH quintics.

The complex polynomials (3) define a quaternion polynomial

$$\mathcal{A}(\xi) \;=\; \mathcal{A}_0(1-\xi)^2 + \mathcal{A}_1 2(1-\xi)\xi + \mathcal{A}_2\xi^2$$

as $\mathcal{A}(\xi) = \boldsymbol{\alpha}(\xi) + \mathbf{k}\,\boldsymbol{\beta}(\xi)$. Identifying the imaginary unit i with the quaternion element $\mathbf{i}$, and writing $\exp(\gamma\,\mathbf{i}) = \cos\gamma + \sin\gamma\,\mathbf{i}$ for any real γ, interpolation of the end tangents $\mathbf{t}_i$, $\mathbf{t}_f$ yields coefficients $\mathcal{A}_0 = \boldsymbol{\alpha}_0 + \mathbf{k}\,\boldsymbol{\beta}_0$, $\mathcal{A}_2 = \boldsymbol{\alpha}_2 + \mathbf{k}\,\boldsymbol{\beta}_2$ obtained from (19)–(20) as

$$\mathcal{A}_0 \;=\; w\,[\,c_i \exp(\phi_i\,\mathbf{i}) + s_i\,\mathbf{k}\,]\,\exp(\psi_0\,\mathbf{i})\,, \tag{43}$$

$$\mathcal{A}_2 \;=\; w\,[\,c_f \exp(\phi_f\,\mathbf{i}) + s_f\,\mathbf{k}\,]\,\exp(\psi_2\,\mathbf{i})\,, \tag{44}$$

where ψ_0, ψ_2 are free parameters, and to satisfy the arc length constraint the value of w is determined[7] by the smaller root w^2 of the biquadratic equation

[7] Although the sign of w is immaterial, we conventionally choose $w > 0$.

(27) with coefficients (28)–(30). In terms of $\mathcal{A}_0, \mathcal{A}_2$ and the known quantities $\Delta\mathbf{p}, \mathbf{t}_i, \mathbf{t}_f, w^2$ we define the vector

$$\mathbf{d} \;=\; 120\,\Delta\mathbf{p} - 15\,w^2(\mathbf{t}_i + \mathbf{t}_f) + 5\,(\mathcal{A}_0\,\mathbf{i}\,\mathcal{A}_2^* + \mathcal{A}_2\,\mathbf{i}\,\mathcal{A}_0^*)\,, \tag{45}$$

and set $d = |\mathbf{d}|$. Then the coefficient $\mathcal{A}_1$ is determined through interpolation of the end–point displacement $\Delta\mathbf{p}$ by [8, 9] the expression

$$\mathcal{A}_1 \;=\; -\frac{3}{4}\,(\mathcal{A}_0 + \mathcal{A}_2) \;+\; \frac{\sqrt{d}}{4}\;\frac{d\,\mathbf{i} + \mathbf{d}}{|\,d\,\mathbf{i} + \mathbf{d}\,|}\;\exp(\psi_1\,\mathbf{i})\,, \tag{46}$$

where ψ_1 is a free parameter. Once $\mathcal{A}_0, \mathcal{A}_1, \mathcal{A}_2$ are known, the control points $\mathbf{p}_0, \ldots, \mathbf{p}_5$ in the Bézier representation

$$\mathbf{r}(\xi) \;=\; \sum_{i=0}^{5} \mathbf{p}_i \binom{5}{i} (1-\xi)^{5-i}\xi^i$$

of $\mathbf{r}(\xi)$ may be obtained [5] with integration constant $\mathbf{p}_0 = \mathbf{p}_i$ as

$$\begin{aligned}
\mathbf{p}_1 \;&=\; \mathbf{p}_0 \;+\; \frac{1}{5}\,\mathcal{A}_0\,\mathbf{i}\,\mathcal{A}_0^*\,,\\
\mathbf{p}_2 \;&=\; \mathbf{p}_1 \;+\; \frac{1}{10}(\mathcal{A}_0\,\mathbf{i}\,\mathcal{A}_1^* + \mathcal{A}_1\,\mathbf{i}\,\mathcal{A}_0^*)\,,\\
\mathbf{p}_3 \;&=\; \mathbf{p}_2 \;+\; \frac{1}{30}(\mathcal{A}_0\,\mathbf{i}\,\mathcal{A}_2^* + 4\,\mathcal{A}_1\,\mathbf{i}\,\mathcal{A}_1^* + \mathcal{A}_2\,\mathbf{i}\,\mathcal{A}_0^*)\,,\\
\mathbf{p}_4 \;&=\; \mathbf{p}_3 \;+\; \frac{1}{10}(\mathcal{A}_1\,\mathbf{i}\,\mathcal{A}_2^* + \mathcal{A}_2\,\mathbf{i}\,\mathcal{A}_1^*)\,,\\
\mathbf{p}_5 \;&=\; \mathbf{p}_4 \;+\; \frac{1}{5}\,\mathcal{A}_2\,\mathbf{i}\,\mathcal{A}_2^*\,.
\end{aligned} \tag{47}$$

As previously noted [5, p. 600] the various terms $\mathcal{A}_r\,\mathbf{i}\,\mathcal{A}_s$ for $r, s \in \{\,0, 1, 2\,\}$ in (47) depend only on the *differences* $\psi_r - \psi_s$ of the free parameters ψ_0, ψ_1, ψ_2. Thus, we can set $\psi_1 = 0$ in (46) without loss of generality. Note also that the vector $\mathbf{d}$ defined by (45) and its magnitude d depend only on the difference $\psi_0 - \psi_2$. However, it is clear from the first term on the right in (46) that $\mathcal{A}_1$, and hence the interpolant $\mathbf{r}(\xi)$, depend *individually* on ψ_0 and ψ_2.

Hence, the problem of matching end points $\mathbf{p}_i, \mathbf{p}_f$ and tangents $\mathbf{t}_i, \mathbf{t}_f$ in conjunction with a prescribed arc length S admits a two–parameter family of solutions, dependent upon the free variables ψ_0, ψ_2. This outcome may be compared with the standard C^1 Hermite interpolation problem of matching end points $\mathbf{p}_i, \mathbf{p}_f$ and *derivatives* $\mathbf{d}_i = \mathbf{r}'(0)$, $\mathbf{d}_f = \mathbf{r}'(1)$, with unconstrained

arc length, in which the solutions also constitute a two–parameter family [9] dependent on free variables ψ_0, ψ_2 associated with $\mathcal{A}_0, \mathcal{A}_2$.

This coincidence in the number of degrees of freedom is not unexpected. In passing from the C^1 Hermite problem to the G^1 Hermite problem with an arc length constraint, one degree of freedom is lost by the *a priori* imposition of a given arc length, but one degree of freedom is gained from the assumption of equal–magnitude end derivatives, $|\mathbf{r}'(0)| = |\mathbf{r}'(1)|$. However, the existence of interpolants to any given data in the former problem was obvious from the availability of a closed–form solution expression, while in the latter problem the analysis of Section 3 is necessary to establish the existence of a derivative magnitude $w^2 = |\mathbf{r}'(0)| = |\mathbf{r}'(1)|$ consistent with the specified arc length S.

We summarize the preceding results with the following algorithm outline. For brevity, this algorithm only considers solutions for user–specified values of the free parameters ψ_0, ψ_2. It may be exploited as a basic function, called by a procedure to optimize the shape of $\mathbf{r}(\xi)$ with respect to these parameters.

Algorithm

input: initial and final points $\mathbf{p}_i$, $\mathbf{p}_f$ and unit tangents $\mathbf{t}_i$, $\mathbf{t}_f$ satisfying condition (5) with $\Delta\mathbf{p} = \mathbf{p}_f - \mathbf{p}_i$, and desired total arc length $S > |\Delta\mathbf{p}|$

1. identify the spatial rotation R and scale factor $f = |\Delta\mathbf{p}|^{-1}$ that map $\Delta\mathbf{p}$ to the canonical displacement $(1, 0, 0)$;

2. apply R to $\mathbf{t}_i, \mathbf{t}_f$ and $\Delta\mathbf{p}$, and multiply S and $\Delta\mathbf{p}$ by f;

3. determine polar and azimuthal angles (θ_i, ϕ_i) and (θ_f, ϕ_f) of the transformed tangents;

4. compute the coefficients of equation (27) specified by the expressions (21) and (28)–(30) for chosen ψ_0, ψ_2 values;

5. compute the smaller root w^2 of equation (27), and take w to be its positive square root;

6. with the chosen ψ_0, ψ_2 values compute the quaternions $\mathcal{A}_0, \mathcal{A}_2$ defined by (43)–(44);

7. compute the quaternion $\mathcal{A}_1$ defined by (45)–(46) with $\psi_1 = 0$;

8. compute the Bézier control points of $\mathbf{r}(\xi)$ from (47);

9. apply the inverse spatial rotation R^{-1} and scaling f^{-1} to restore the curve $\mathbf{r}(\xi)$ to its original size and orientation.

output: spatial PH quintic $\mathbf{r}(\xi)$ satisfying $\mathbf{r}(0) = \mathbf{p}_i$, $\mathbf{r}(1) = \mathbf{p}_f$, and $\mathbf{r}'(0) = |\mathbf{r}'(0)|\,\mathbf{t}_i$, $\mathbf{r}'(1) = |\mathbf{r}'(1)|\,\mathbf{t}_f$ with total arc length S.

Remark 2. For given ψ_0, ψ_2 values the algorithm involves — besides rational arithmetic — only trigonometric function evaluations and (real) square root extractions, and is therefore amenable to exact implementation in a symbolic computation system accommodating these functions. For brevity, we present below only examples computed in floating–point arithmetic — note also that the shape optimization process generally requires a numerical solution.

To characterize the shape quality of the interpolant $\mathbf{r}(\xi)$, we consider the "bending energy" — i.e., the integral of the square of the curvature κ with respect to arc length s,

$$E \;=\; \int_0^S \kappa^2 \,\mathrm{d}s\,. \tag{48}$$

E is proportional the strain energy stored in an initially–straight thin elastic rod that is bent into the curve shape. Curves minimizing E, subject to given geometrical constraints, are generally considered to be of "optimum" shape. For a parametric space curve $\mathbf{r}(\xi)$, the curvature is defined [13] by

$$\kappa(\xi) \;=\; \frac{|\,\mathbf{r}'(\xi) \times \mathbf{r}''(\xi)\,|}{|\,\mathbf{r}'(\xi)\,|^3}\,,$$

The integral (48) may be simplified by noting that every spatial PH curve satisfies [10] the relation

$$|\mathbf{r}'(\xi) \times \mathbf{r}''(\xi)|^2 \;=\; \sigma^2(\xi)\,\rho(\xi)\,,$$

where the polynomial $\rho(\xi)$ may be expressed in terms of the Hopf map form (4) as

$$\rho(\xi) \;=\; 4\,|\,\boldsymbol{\alpha}(\xi)\boldsymbol{\beta}'(\xi) - \boldsymbol{\alpha}'(\xi)\boldsymbol{\beta}(\xi)\,|^2\,.$$

Since $\mathrm{d}s = \sigma(\xi)\,\mathrm{d}\xi$, the expression (48) reduces to

$$E \;=\; 4\int_0^1 \frac{|\,\boldsymbol{\alpha}(\xi)\boldsymbol{\beta}'(\xi) - \boldsymbol{\alpha}'(\xi)\boldsymbol{\beta}(\xi)\,|^2}{\sigma^3(\xi)}\,\mathrm{d}\xi\,. \tag{49}$$

For PH quintics, the integrand has a quartic numerator, and the cube of the parametric speed as denominator. By computing the roots of $\sigma(\xi)$, which is

also quartic, the integral admits a closed–form reduction by partial–fraction decomposition of the rational integrand. Alternatively, an adaptive numerical quadrature — such as the Simpson rule [14] — yields rapid convergence to machine precision, since the integrand is non–negative.

It should be noted that imposition of a specified arc length S on the curve $\mathbf{r}(\xi)$ plays an important role in the minimization of (48). Curves minimizing E under given boundary conditions, but without constraining the arc length, need not be finite [1], since loops of length $S \sim 2\pi r$ and curvature $\kappa \sim 1/r$ satisfy $E \to 0$ as $r \to \infty$. The present construction eliminates this concern.[8]

The integral (49) has a rather complicated dependence on the parameters ψ_0 and ψ_2, and determining its derivatives with respect to them is clearly a non–trivial task. The use of optimization techniques that do not depend on derivative information [2] may therefore be preferable.

Some simpler methods for identifying values for the free parameters ψ_0, ψ_2 so as to generate C^1 PH quintic Hermite interpolants with good shape quality were proposed in [9]. Since the imposition of an arc length constraint amounts to fixing a common end derivative magnitude through the solution of equation (27), these methods should also be applicable in the present context.

Example 1. For the data

$$S \;=\; 1.25\,, \quad (\theta_i, \phi_i) \;=\; (0.65\,\pi, -0.25\,\pi)\,, \quad (\theta_f, \phi_f) \;=\; (0.25\,\pi, 0.25\,\pi)\,,$$

together with parameter values $\psi_0 = 1.00\,\pi$ and $\psi_2 = 0.00\,\pi$, the smaller root of (27) yields the value

$$w \;=\; 0.928517\,.$$

The corresponding coefficients of the complex polynomials (10) are

$$\begin{aligned}
\boldsymbol{\alpha}_0 &= -0.343052 + 0.343052\,\mathrm{i}\,, & \boldsymbol{\beta}_0 &= -0.791691 + 0.000000\,\mathrm{i}\,,\\
\boldsymbol{\alpha}_1 &= -0.197648 + 2.031303\,\mathrm{i}\,, & \boldsymbol{\beta}_1 &= 0.305611 - 0.235042\,\mathrm{i}\,,\\
\boldsymbol{\alpha}_2 &= 0.606583 + 0.606583\,\mathrm{i}\,, & \boldsymbol{\beta}_2 &= 0.355328 + 0.000000\,\mathrm{i}\,,
\end{aligned}$$

and the quaternion coefficients $\mathcal{A}_i = \boldsymbol{\alpha}_i + \mathbf{k}\,\boldsymbol{\beta}_i$ are

$$\begin{aligned}
\mathcal{A}_0 \;&=\; -0.343052 + 0.343052\,\mathbf{i} + 0.000000\,\mathbf{j} - 0.791691\,\mathbf{k}\,,\\
\mathcal{A}_1 \;&=\; -0.197648 + 2.031303\,\mathbf{i} - 0.235042\,\mathbf{j} + 0.305611\,\mathbf{k}\,,\\
\mathcal{A}_2 \;&=\; 0.606583 + 0.606583\,\mathbf{i} + 0.000000\,\mathbf{j} + 0.355328\,\mathbf{k}\,.
\end{aligned}$$

[8] Since, for given G^1 Hermite data, the equation (27) and coefficients (28)–(30) establish a unique relation between the derivative magnitude w^2 and total arc length S, this is also true for C^1 PH quintic Hermite interpolants that have equal end derivative magnitudes.

The curve control points are determined from (47) as

$$\begin{aligned}
\mathbf{p}_0 &= (0.000000, 0.000000, 0.000000)\,, \\
\mathbf{p}_1 &= (-0.078281, 0.108636, -0.108636)\,, \\
\mathbf{p}_2 &= (0.123038, 0.102837, -0.425427)\,, \\
\mathbf{p}_3 &= (0.677340, -0.080730, -0.296160)\,, \\
\mathbf{p}_4 &= (0.878075, -0.086214, -0.086214)\,, \\
\mathbf{p}_5 &= (1.000000, 0.000000, 0.000000)\,.
\end{aligned}$$

Figure 2 shows the resulting interpolant: the curve end tangents and total arc length, computed in double–precision arithmetic, agree with the prescribed data to an accuracy of $\sim 10^{-15}$. For the specified end points, end tangents, and ψ_0, ψ_2 values, Figure 2 also illustrates the interpolants for the sequence of arc lengths $S = 1.1, 1.2, 1.3, 1.4, 1.5$ — the corresponding w values are found to be $0.597709, 0.835205, 1.011615, 1.156157, 1.280351$.

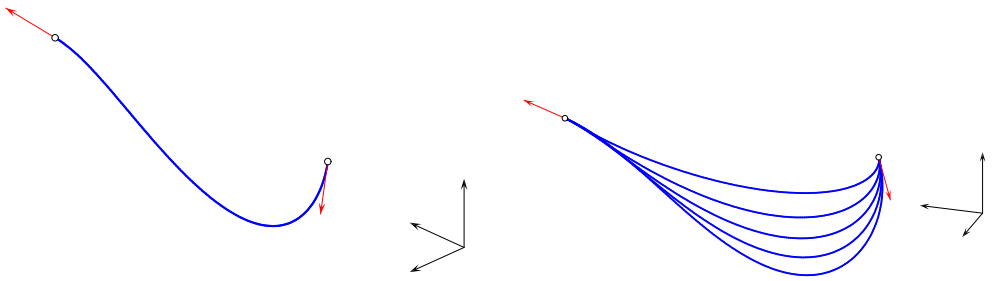

Figure 2: Left: a quintic PH curve satisfying the data specified in Example 1. Right: instances of this curve with given arc lengths $S = 1.1, 1.2, 1.3, 1.4, 1.5$.

This example is also used to illustrate the sensitivity of the interpolants to the free parameters ψ_0, ψ_2. Figure 3 shows the families of curves obtained for $\psi_0 = k\,\pi/4$, $k = 0, \ldots, 7$ with $\psi_2 = 0$, and for $\psi_0 = 0$ with $\psi_2 = k\,\pi/4$, $k = 0, \ldots, 7$. The influence of ψ_0, ψ_2 on the curve shape is clearly apparent.

Example 2. For the data

$$S = 1.50\,, \quad (\theta_i, \phi_i) = (-0.25\,\pi, -0.25\,\pi)\,, \quad (\theta_f, \phi_f) = (0.25\,\pi, -0.25\,\pi)\,,$$

solutions were computed for a dense sampling of parameter values $(\psi_0, \psi_2) \in [\,0, 2\pi) \times [\,0, 2\pi)$. The minimum energy solution with $E \approx 10.475$, shown in

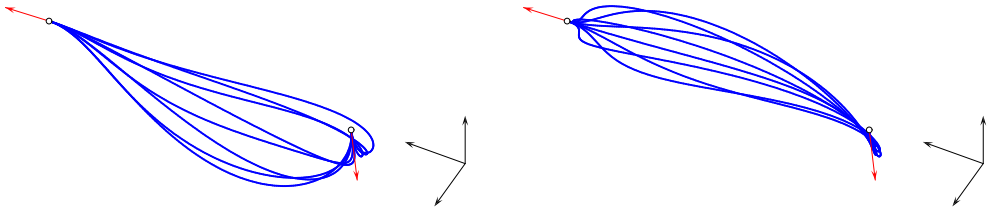

Figure 3: The curve in Example 1 with arc length $S = 1.25$, using different values of the parameters ψ_0, ψ_2. Left: the curves obtained with $\psi_0 = k\,\pi/4$, $0 \leq k \leq 7$ and $\psi_2 = 0$. Right: curves with $\psi_0 = 0$ and $\psi_2 = k\,\pi/4$, $0 \leq k \leq 7$.

Figure 4, was observed at $(\psi_0, \psi_2) \approx (0.14\,\pi, 0.86\,\pi)$ corresponding to $w \approx 1.8512$. However, a maximum energy $E \approx 2697.7$ was also observed among the solutions, at $(\psi_0, \psi_2) \approx (1.47\,\pi, 0.69\,\pi)$ corresponding to $w \approx 2.3329$. The minimum–energy solution exhibits the modest extremum curvature $\kappa_{\max} \approx 3.805$, but $\kappa_{\max} \approx 1016.2$ for the maximum–energy case.

It should be noted that the quantity w, which specifies the magnitude of the end derivatives, is not the primary determinant of the bending energy E and shape of the interpolant. In the present case, this quantity was found to vary over the quite modest range $1.6635 \lesssim w \lesssim 2.3525$, and the extremes of this range do not identify the minimum and maximum energy interpolants. The angular parameters ψ_0, ψ_2 appear to have the strongest influence on the interpolant shapes. Analogous parameters occur [8, 9] in the problem of C^1 Hermite interpolation by spatial PH quintics, which differs from the present context in that (i) *magnitudes* (not just directions) are specified for the end derivatives; and (ii) there is no constraint on the arc length. Some practical rules for selecting these angular parameters were proposed in [9].

Although all choices of the ψ_0, ψ_2 parameter values yield formally correct interpolants to the prescribed end points, end tangents, and arc length, this example illustrates their strong influence on the interpolant shape, and the importance of determining them through an optimization scheme, to ensure solutions of desirable shape. A comprehensive analysis of the dependence of the curve shape on ψ_0 and ψ_2, in order to gain greater insight and develop more deterministic methods for their selection, is clearly desirable. However, this is a non–trivial problem, beyond the scope of the present study.

Finally, we make use of this example to illustrate the fact that, although the existence proof depends only on the *difference* $\Delta\psi = \psi_2 - \psi_0$ of the free parameters ψ_0 and ψ_2, the interpolant shape depends on them *individually*. Figure 4 illustrates the solutions obtained with $(\psi_0, \psi_2) = (0.2\,\pi, 1.0\,\pi)$ and

$(\psi_0, \psi_2) = (0.4\,\pi, 1.2\,\pi)$. Although both cases correspond to $\Delta\psi = 0.8\,\pi$, the resulting interpolants are seen to be distinct.

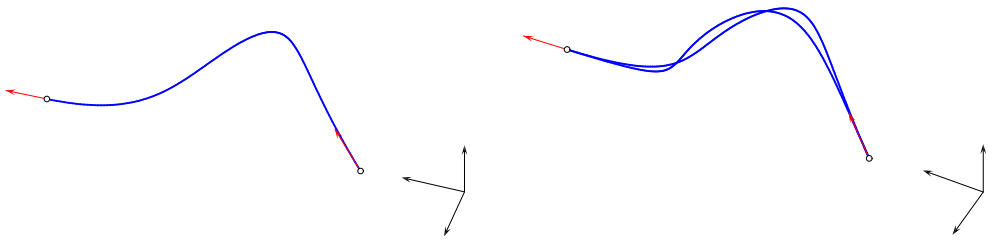

Figure 4: Left: a quintic PH curve satisfying the data specified in Example 2. Right: comparison of two PH quintic interpolants constructed with the same end points, tangents, and arc lengths (as defined in Example 2) using different individual ψ_0, ψ_2 values that have the same difference $\Delta\psi = \psi_2 - \psi_0$.

5 Closure

The distinctive algebraic structures of Pythagorean–hodograph curves permit exact constructions of spatial paths that satisfy given boundary constraints and possess prescribed arc lengths. The present study addresses the existence of PH quintic interpolants with specified (non–planar) end point and tangent data, and a desired total arc length. Because of the non–linear nature of the construction, the existence of solutions for arbitrary consistent data sets is non–obvious. Nevertheless, it was established that solutions do exist for any data, and in fact they always constitute a two–parameter family.

Under the assumption of equal–magnitude end derivatives (which ensures that symmetric data yields symmetric interpolants), the question of existence was reduced to determining whether or not a certain biquadratic equation with data–dependent coefficients always admits a positive real root satisfying certain data–dependent bounds. It was possible to address this affirmatively, based on certain inequality and sign arguments, without the need to explicitly solve the equation. In fact, the interpolants are seen to depend on two free angular parameters, which may be exploited for shape optimization.

The practical consequences of the analysis presented herein are as follows: (i) the arc–length–constrained G^1 PH quintic Hermite interpolation problem can be tackled with confidence in the knowledge that solutions exist for any

given data; (ii) the results essentially provide a simple method to determine the end–derivative magnitude that achieves the prescribed arc length — once determined, existing methodology for constructing PH quintic interploants can be exploited; and (iii) the dependence of the interpolants upon two free variables, which can be used as shape parameters, has been established.

The focus of this study has been to establish the existence of interpolants to G^1 Hermite data with prescribed arc lengths. Because of their non–linear influence on the final curve shape, a systematic analysis of the role of the two free parameters ψ_0, ψ_2 is a non–trivial task, that is best deferred to a separate in–depth study. On a practical level, numerical optimization schemes can be used to identify the ψ_0, ψ_2 values that minimize the bending energy, although this can be rather computation–intensive.

References

[1] G. Birkhoff and C. de Boor (1965), Piecewise polynomial interpolation and approximation, in *Approximation of Functions* (H. L. Garabedian, ed.), Elsevier, Amsterdam, 164–190.

[2] R. P. Brent (1973), *Algorithms for Minimization Without Derivatives* Dover (reprint), Mineola, NY.

[3] H. I. Choi and C. Y. Han (2002), Euler–Rodrigues frames on spatial Pythagorean–hodograph curves, *Comput. Aided Geom. Design* **19**, 603–620.

[4] H. I. Choi, D. S. Lee, and H. P. Moon (2002), Clifford algebra, spin representation, and rational parameterization of curves and surfaces, *Adv. Comp. Math.* **17**, 5–48.

[5] R. T. Farouki (2008), *Pythagorean–Hodograph Curves: Algebra and Geometry Inseparable*, Springer, Berlin.

[6] R. T. Farouki (2016), Construction of G^1 planar Hermite interpolants with prescribed arc lengths, *Comput. Aided Geom. Design* **46**, 64–75.

[7] R. T. Farouki, M. al–Kandari, and T. Sakkalis (2002), Structural invariance of spatial Pythagorean hodographs, *Comput. Aided Geom. Design* **19**, 395–407.

[8] R. T. Farouki, M. al–Kandari, and T. Sakkalis (2002), Hermite interpolation by rotation–invariant spatial Pythagorean–hodograph curves, *Adv. Comp. Math.* **17**, 369–383.

[9] R. T. Farouki, C. Giannelli, C. Manni, and A. Sestini (2008), Identification of spatial PH quintic Hermite interpolants with near–optimal shape measures, *Comput. Aided Geom. Design* **25**, 274–297.

[10] R. T. Farouki, C. Giannelli, and A. Sestini (2009), Helical polynomial curves and double Pythagorean hodographs I. Quaternion and Hopf map representations, *J. Symb. Comput.* **44**, 161–179.

[11] M. Huard, R. T. Farouki, N. Sprynski, and L. Biard (2014), C^2 interpolation of spatial data subject to arc–length constraints using Pythagorean–hodograph quintic splines, *Graph. Models* **76**, 30–42.

[12] M. Krajnc (2017), Interpolation with spatial rational Pythagorean–hodograph curves of class 4, *Comput. Aided Geom. Design* **56**, 16–34.

[13] E. Kreyszig (1959), *Differential Geometry*, University of Toronto Press.

[14] J. Stoer and R. Bulirsch (2002), *Introduction to Numerical Analysis*, 3rd Edition, Springer, New York.

[15] J. V. Uspensky (1948), *Theory of Equations*, McGraw–Hill, New York.